NON-NEWTONIAN FLUID FLOW THROUGH A STAGGERED SQUARE TUBE BANK

By

CARLYN GRANT CRUZAN

Bachelor of Science

University of Oklahoma

Norman, Oklahoma

1961

Submitted to the faculty of the Graduate School
of the Oklahoma State University
in partial fulfillment of the requirements
for the degree of
MASTER OF SCIENCE
August, 1964

NON-NEWTONIAN FLUID FLOW THROUGH

A STAGGERED SQUARE TUBE BANK

Thesis Approved:

Kenneth L Bell
Thesis Advisor

R. N. Maddox

Dean of the Graduate School

PREFACE

A method is proposed to apply Reynolds number-friction factor diagrams for Newtonian flow through a tube bank to use for non-Newtonian pseudoplastic flow through similar tube banks. Experimental data were taken to support the arguments. Also included is a discussion of non-Newtonian pseudoplastic flow through an orifice. In Appendix B, a derivation is presented to determine rheological constants for pseudoplastic non-Newtonian fluids. The derivation is based on the empirical Ostwald-de Waele power law for non-Newtonian fluids. This method was used to analyze and correlate the experimental data.

Many people have given me guidance and assistance during the course of my study. Particular gratitude is extended to Dr. R. N. Maddox, Dr. R. W. MacVicar, Dr. J. B. West, and Dean D. K. Troxel for their efforts extended in my behalf far beyond the demands of their academic functions. I am indebted to Dr. K. J. Bell, my advisor, for his aid and suggestions in relation to my thesis work. Professor A. G. Comer provided me with a number of helpful references and also the use of a Fann V-G Viscometer. My parents have provided me with a wealth of moral support. Mrs. Arleen Fairchild was very helpful in assisting me with the mechanical construction of the thesis. The assistance of Robert L. Robinson who aided me in numerous tasks involved in this work was greatly appreciated. The Driscose (sodium carboxymethylcellulose) was furnished by the Drilling Specialities Company of Bartlesville, Oklahoma, which is a subsidiary of Phillips

Petroleum Company. Oklahoma State University provided me with an institutional assistantship and experimental facilities.

TABLE OF CONTENTS

LIST OF TABLES

CHAPTER I

INTRODUCTION

A process that is common to almost every chemical plant and refinery is that of heating and cooling fluids. Experience has shown that the heating and cooling of fluids is achieved most economically in a large number of applications by shell and tube heat exchangers. Work is constantly being done to make the shell and tube heat exchanger more efficient and to make its design more exact. One factor that determines what size of heat exchanger is needed for a specific application is the amount of work (energy loss) needed to force a fluid through the heat exchanger. There are energy losses on both the shell and the tube sides of the exchanger.

The shell side of an exchanger contains baffles supporting rows of tubes. These baffles direct the flow of the fluid perpendicular to the axes of the tubes on the shell side of the exchanger. Tube banks simulate one crossflow section of a baffled heat exchanger under conditions of uniform flow with no leakage. There are energy losses in each baffled section that contribute to the total energy loss on the shell side of the exchanger. Attempts by other authors have been made to predict the amount of energy loss as the fluid flows through one of these baffled sections.

Many fluids do not obey the Newtonian viscosity law which states that the shear rate is proportional to the shear stress; these are

called non-Newtonian fluids. For non-Newtonian fluids, it becomes necessary to obtain new information whereby a designer can have some basis for designing shell and tube heat exchangers by providing a basis for calculation of energy losses. This thesis is intended to be a contribution to the designer who encounters non-Newtonian flow on the shell side of shell and tube heat exchangers by providing a basis for calculation of energy losses.

CHAPTER II

LITERATURE SURVEY

Tube banks are often constructed to simulate one crossflow section of a baffled heat exchanger under conditions of uniform flow with no leakage (1). One of the primary problems confronting the heat exchanger designer is the problem of computing the pressure drop on the shell side of the exchanger. Boucher and Lapple have listed in a paper (2) some of the variables that affect pressure drop in tube banks. Selected variables applicable to the conditions considered in this study from the Boucher and Lapple paper are listed below:

VARIABLES AFFECTING PRESSURE DROP ACROSS TUBE BANKS

I. Primary variables
   - A. Operating conditions
     1. Fluid flow rates
     2. Fluid characteristics or properties
   - B. Tube-bank arrangements
     1. Tube spacing (transverse and longitudinal)
     2. Tube alignment characteristics (in-line or staggered)

II. Secondary variables
   - A. Fluid approach configuration
   - B. Tube surface characteristics: roughness
   - C. Mutual effect of tube rows on each other

Some of the more important variables will be discussed.

Tube Bank Arrangements

There are many types of tube arrangements. Each arrangement satisfies some specific engineering need. Some of the more commonly used tube arrangements are drawn in Figure 1 on page 5.

The tube pitch is defined as the shortest center-to-center distance between adjacent tubes. The tube clearance is the shortest distance between adjacent tubes. Another common term used in the study of tube banks is that of the pitch ratio. The pitch ratio is defined as the ratio of the pitch to the outside diameter.

Fluid Characteristics

Newton's law of viscosity is a mathematical model describing how a fluid reacts to an applied shear force. A plot of the shear stress $\tau_{r\theta}$ versus the shear rate $\frac{r d\left(\frac{V_\theta}{r}\right)}{dr}$ (*) for a Newtonian fluid gives a straight line that terminates at the origin. The slope of this line is termed the viscosity and is constant throughout the entire range of shear rates for a Newtonian fluid. Newtonian flow characteristics are approached by gases and liquids of relatively low molecular weights. The shear stress-shear rate equation is

$$\tau_{r\theta} = \mu \frac{r d\left(\frac{V_\theta}{r}\right)}{dr} \qquad (1)$$

where μ is the viscosity and is a constant for Newtonian fluids.

Most fluids show some degree of non-Newtonian characteristics. The slope at a particular shear rate is called the apparent viscosity. If the apparent viscosity decreases with increasing shear rate, the non-Newtonian fluid is called a pseudoplastic; if the apparent viscosity increases with increasing shear rate, the non-Newtonian fluid is called

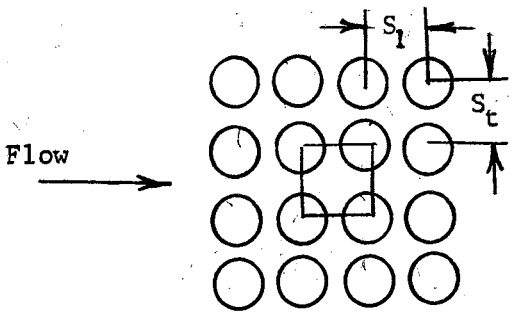

(a) Inline Square Pitch

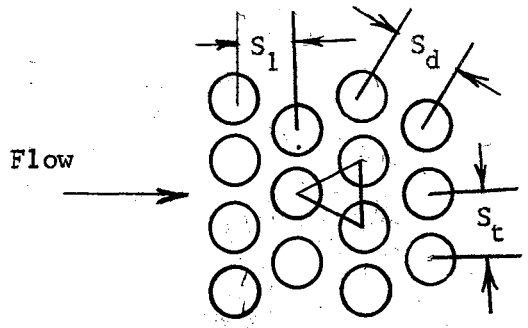

(b) Triangular Pitch

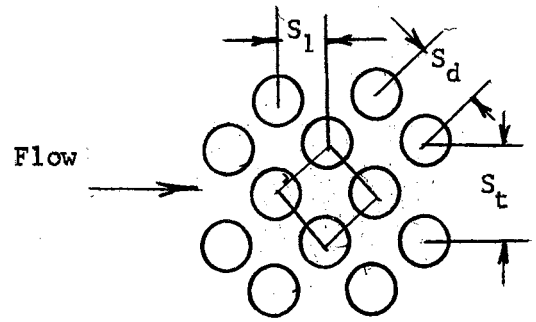

(c) Staggered Square Pitch

Figure 1. Common Tube Layouts

dilatant. Figure 2 on page 7 is a shear stress-shear rate diagram. Pseudoplastic fluids are of primary interest in this work.

There are many empirical equations that have been proposed to represent pseudoplastic shear stress-shear rate relationships (3, 4, 5). Ostwald-de Waele (6) have presented one of the most widely accepted shear stress-shear rate relationships. This is the empirical power function relationship

$$\tau_{r\theta} = K \left[\frac{r d\left(\frac{V_\theta}{r}\right)}{dr} \right]^{n'} \tag{2}$$

K and n' are constants that are evaluated empirically. See Appendix B.

A water solution of high viscosity Driscose (sodium carboxymethylcellulose) was the non-Newtonian fluid selected for this thesis. Sodium carboxymethylcellulose-water solution is a pseudoplastic non-Newtonian fluid. The apparent viscosity of this fluid is approximately 2,000 centipoises (7) at low shear rates. Sodium carboxymethylcellulose is a generic name for a number of methylated cellulose sodium salts.

Fluid Flow Rates

The most generally accepted method of correlating pressure drop information from pipes and tube banks is by means of friction factor-Reynolds number diagrams. The Reynolds number of a Newtonian fluid for flow through a pipe is

$$Re_p = \frac{D_i V_p \rho}{\mu} \tag{3}$$

The commonly used Reynolds number for Newtonian flow through tube banks is

$$Re_t = \frac{D_t V_t \rho}{\mu} \tag{4}$$

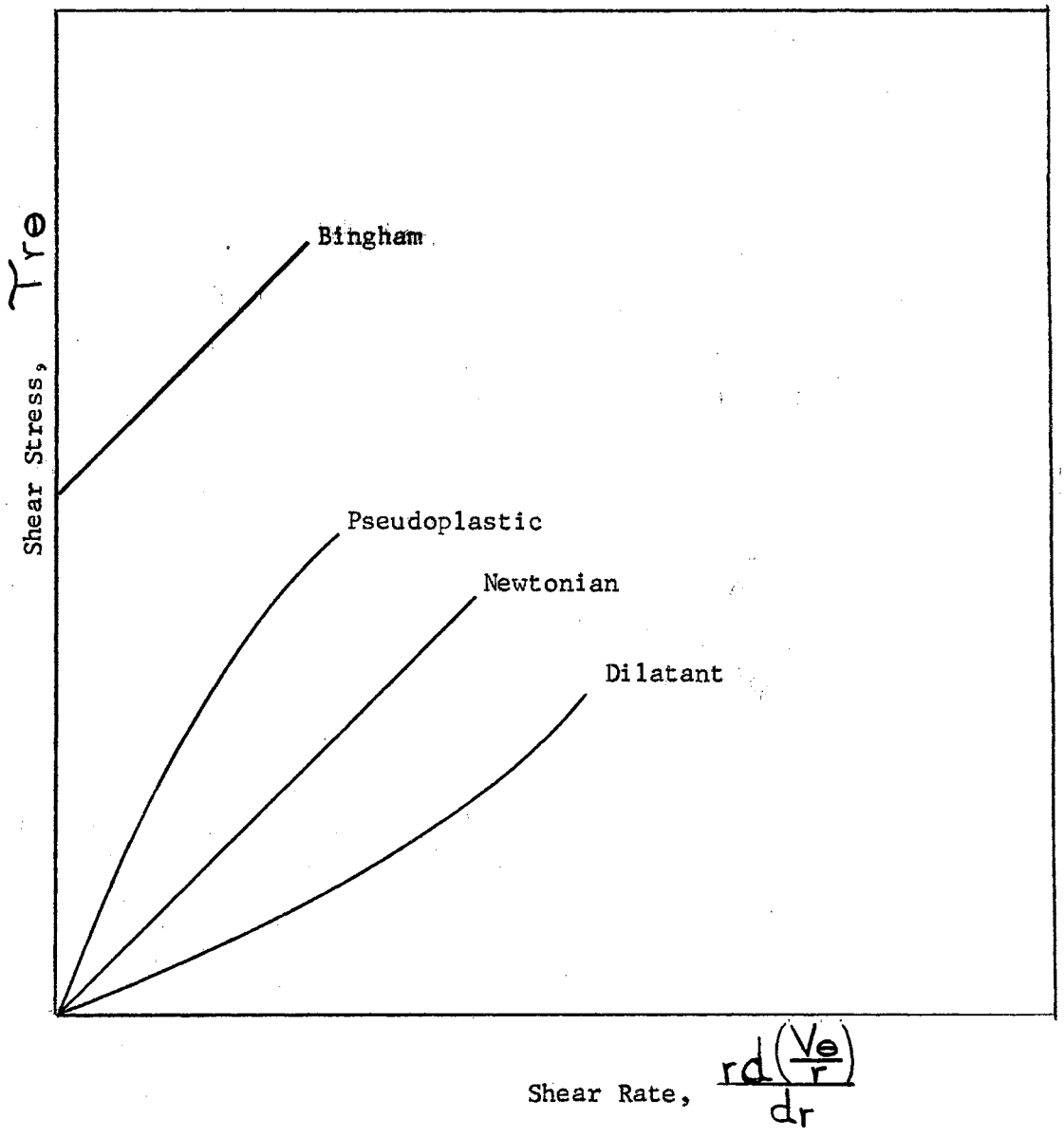

Figure 2. Shear Stress-Shear Rate Diagram

There are two differences between terms of equations (3) and (4). The first difference is that the D_t for the tube bank is the outside diameter of the tube, whereas the D_i for the pipe is the inside diameter of the pipe. The second difference is in the velocity terms. The velocity term for the tube bank is the velocity at the minimum area for flow (maximum velocity). The velocity term for the pipe is the average velocity in the pipe.

The Reynolds number for flow through a pipe was derived by a dimensional analysis procedure. The density (ρ) and the viscosity terms (μ) are characteristic of the fluid flowing through the pipe. The diameter of the pipe (D_i) and the fluid velocity (V_p) are characteristic of the mechanical system. The derivation of the Reynolds number does not specify that the characteristic length of a system must be a diameter but any dimension that will describe the system. Also the derivation of the Reynolds number does not specify that the characteristic velocity of a system must be a pipe velocity but any velocity that will describe the system. Equation (4) is a transformation of equation (3) justified by dimensional analysis.

There are two serious drawbacks that arise in the use of equation (4). The first drawback is that there is no allowance for the different types of tube arrangements encountered, and the second drawback is that there is no allowance for the difference in pitch ratios. Consequently, for each different tube layout and each different pitch ratio there must be a separate friction factor-Reynolds number curve.

Metzner and Reed (8) have derived a Reynolds number for a non-Newtonian fluid flowing through a pipe. This equation is based on the applicability of the Ostwald-de Waele empirical power function relation-

ship between shear stress and shear rate, equation (2). The Metzner-Reed Reynolds number derived by dimensional analysis is

$$Re_P = \frac{D_i^{n'} V_P^{2-n'} \rho}{\gamma} \tag{5}$$

where γ is evaluated by

$$\gamma = g_c K' 8^{n'-1} \tag{6}$$

K' in the above equation is defined by

$$K' = K \left(\frac{3n'+1}{4n'} \right)^{n'} \tag{7}$$

Evaluation of K' and n' is discussed in Appendix B.

The subject of concern is whether or not the Reynolds number-friction factor diagrams for the flow of a Newtonian fluid across a tube bank can be applied to non-Newtonian fluids flowing across a similar tube bank. The Reynolds number must be modified to apply to non-Newtonian flow. This modification will be analogous to the modification in which equation (3) was modified to give equation (4). The proposed equation for pseudoplastic non-Newtonian flow through a tube bank is

$$Re_t = \frac{D_o^{n'} V_t^{2-n'} \rho}{\gamma} \tag{8}$$

A matter of secondary concern is whether or not the Reynolds number-orifice coefficient diagram for the flow of a Newtonian fluid flowing through an orifice can be applied to non-Newtonian fluids flowing through a similar orifice. The Reynolds number equation for an orifice for non-Newtonian flow will be the same as equation (8) except for changing D_o to D_{or} and changing V_t to V_p. This equation is

then

$$Re_{OR} = \frac{D_{OR}^{n'} V_{OR}^{2-n'} \rho}{\gamma} \tag{9}$$

Friction Factor

A number of friction factors have been defined in the literature (9, 10). The Chilton-Genereaux form of the friction factor will be used to correlate experimental data in this thesis. The Chilton-Genereaux friction factor is

$$f = \frac{2\Delta P g_c \rho}{4 G_m^2 N} \tag{10}$$

Orifice Coefficient for Non-Newtonian Flow

An orifice, Figure 3, is a sharp-edged aperture of smaller diameter than the supply main through which the fluid is flowing. The purpose of an orifice is to create a pressure drop which can be measured and related to flow rate. An orifice meter is a system containing an orifice and a differential pressure indicating device. The general orifice coefficient definition (11) for incompressible fluids in plug flow is

$$C_o = \frac{V_P}{\sqrt{\frac{2 g_c \left(\frac{-\Delta P}{\rho}\right)}{\frac{S_1^2}{S_o^2} - 1}}} \tag{11}$$

There are permanent energy losses in an orifice meter as a result of the viscous dissipation of energy. The viscosity of Newtonian fluids remains constant throughout any range of shear rates. Pseudoplastic

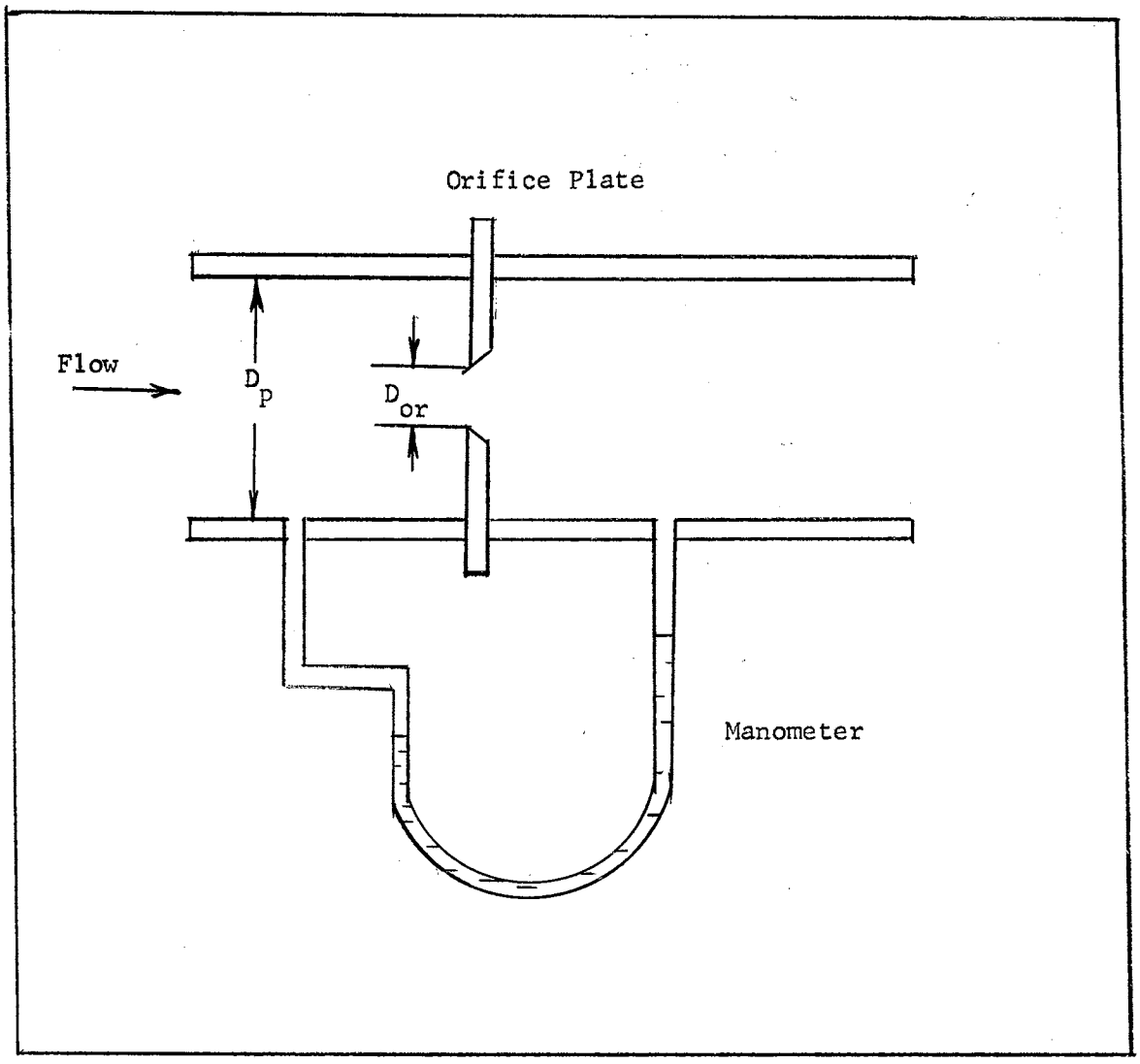

Figure 3. Schematic Diagram of an Orifice Meter

non-Newtonian fluids have a high apparent viscosity at low shear rates and low viscosity at high shear rates. The difference in viscosities of the pseudoplastic non-Newtonian fluids at different shear rates indicate that the faster a fluid flows past a stationary surface, the lower its apparent viscosity.

There are three distinct zones where viscous dissipation of energy occurs during flow of a fluid through an orfice. The first zone is in the main stream on the upstream side of the orifice. The second zone is in the main stream on the downstream side of the orifice. The third is the eddy zone on the downstream side of the orifice. During turbulent flow most of the viscous dissipation of the system is in the eddy zone. The eddy zone dissipation is relatively less for pseudoplastic fluids than for Newtonian fluids.

The viscosity of the Newtonian fluids flowing through an orifice is constant and is the same in all three zones previously described. The apparent viscosity of a pseudoplastic non-Newtonian fluid flowing through an orifice has three different values due to the different shear rates. These different apparent viscosities have an effect on the viscous dissipation of energy which in turn contributes to the overall pressure drop. The orifice coefficient is a function of the overall pressure drop. The difference in viscosity due to non-Newtonian flow as compared to the constant viscosity of Newtonian fluids would indicate that the orifice coefficients of the two types of fluids at corresponding Reynolds numbers might have different values. This reasoning would indicate that equation (9) could be a valid representation of the Reynolds number for non-Newtonian pseudoplastic flow through an orifice, but the orifice coefficient definition should also be modified for non-Newtonian

fluids. If so, an orifice coefficient diagram for Newtonian fluids flowing through an orifice could not be used for non-Newtonian fluids without modification.

(*) Shear stress-shear rate relationships are expressed in terms of cylindrical coordinates in this work because the constants of shear stress-shear rate equations are determined by methods based on a rotational viscometer. A discussion of shear stress-shear rate relationships are found in Appendix B.

CHAPTER III

EXPERIMENTAL APPARATUS

The apparatus consisted of two tube banks, a liquid circulating system, an orifice, and two fluid-filled U-tube manometers. Figure 4 on page 15 is a schematic diagram of the experimental apparatus. The tube bank was vertically oriented to reduce the possibility of air entering the tube bank manometer lines and interfering with the manometer readings. A Fann V-G viscometer was used to evaluate rheological constants.

Tube Banks

The tube banks, Figure 5 on page 16, were encased in a rectangular brass conduit 4 inches long, 2 inches high, and 1.856 inches wide. The "tubes" were made of 0.250 inch O. D. brass rods. The tube-sheet layout was a staggered square with a pitch ratio of 1.5. Two different tube banks were used in this experiment, each with 3.5 tubes per row. One tube bank contained four tube rows and the second contained eight tube rows in the longitudinal direction.

Liquid Circulating System

The pump was a Moyno 1L6, type CDQ, positive displacement pump powered by a 3 horsepower motor. Flow rates were controlled by a variable speed drive attached to the motor. The angular velocity of the pump

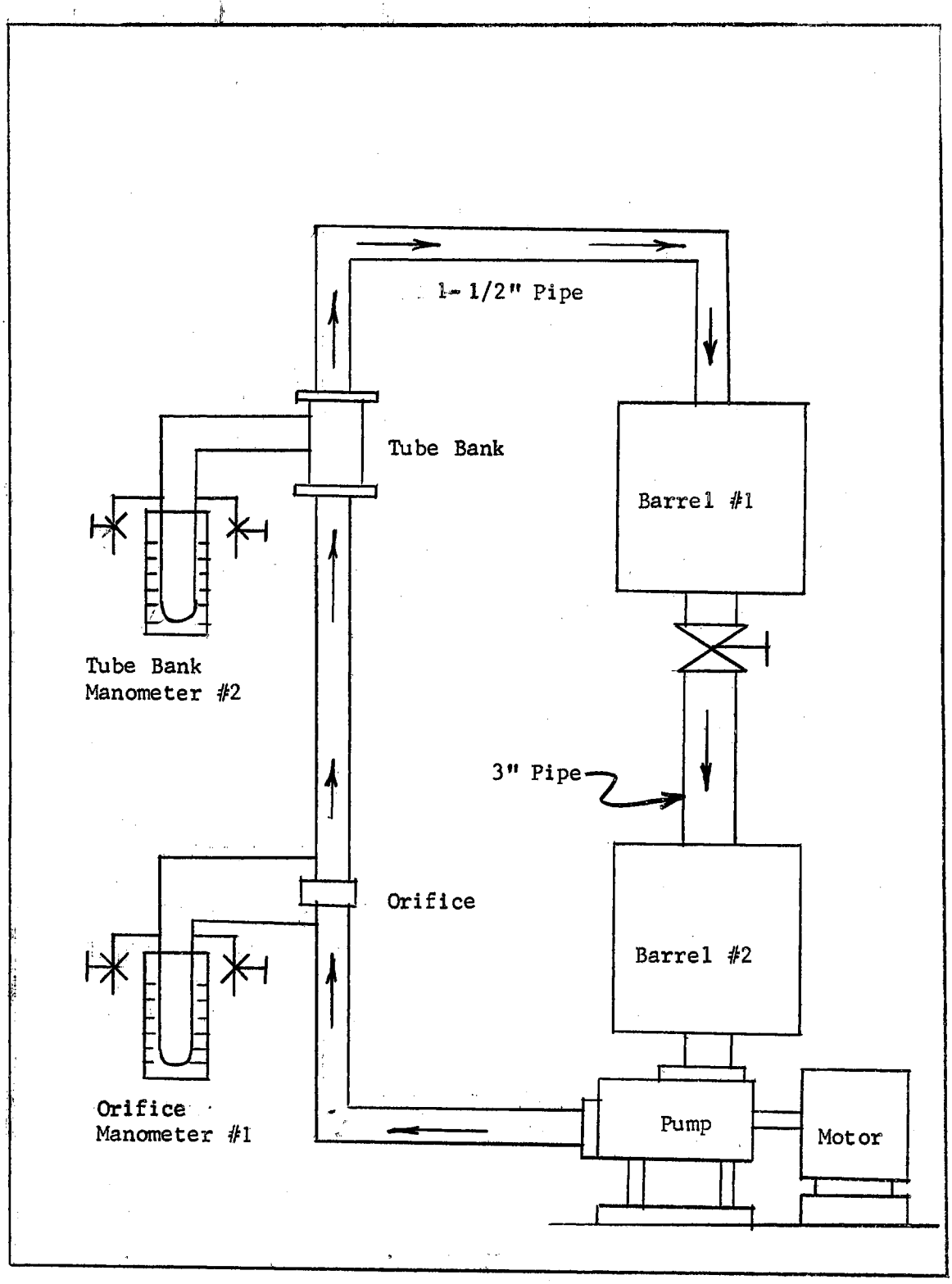

Figure 4. Schematic Diagram of Flow Apparatus

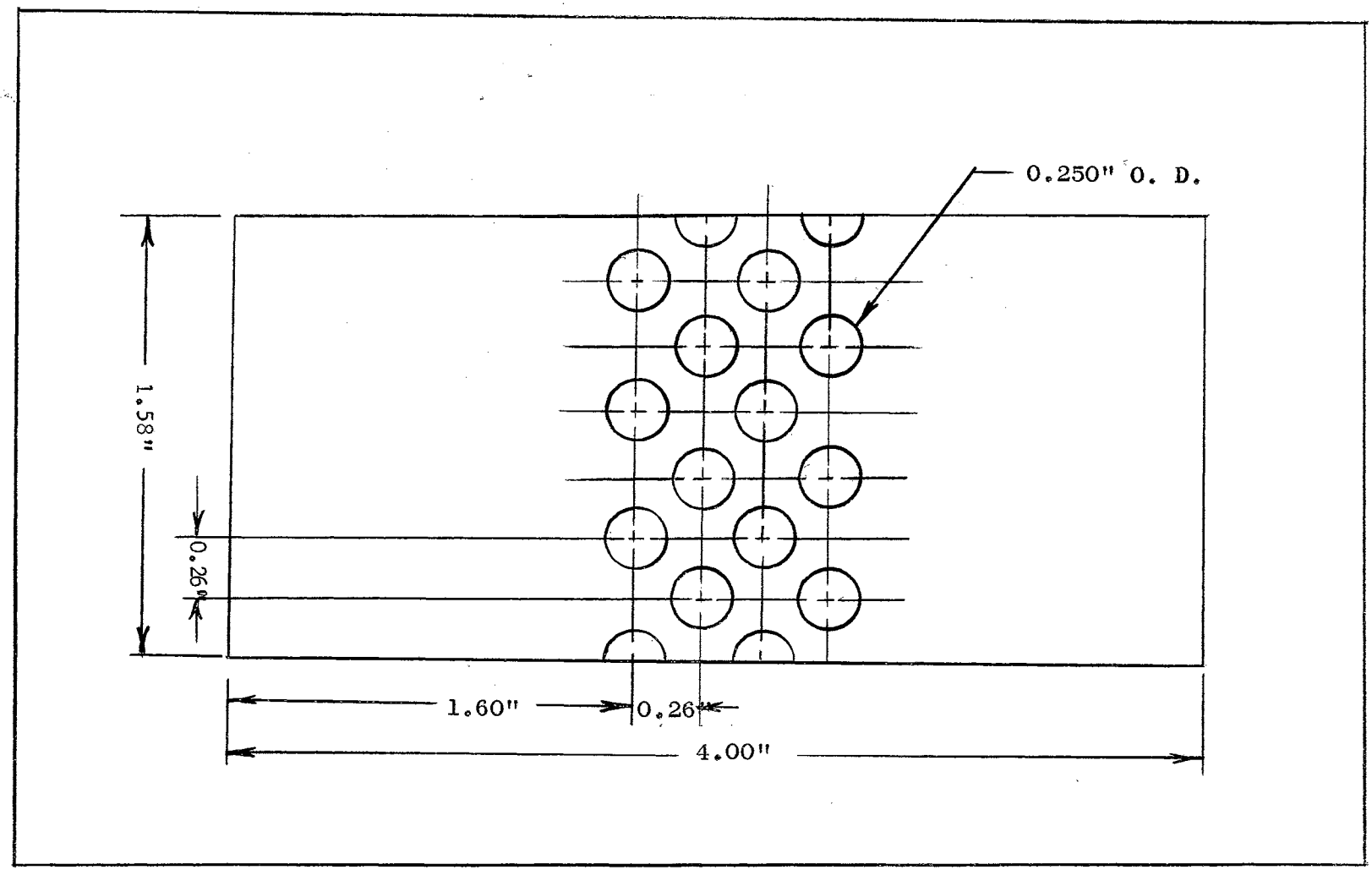

Figure 5. Schematic Diagram of Tube Bank

rotor varied from 85 to 665 revolutions per minute. The output of the pump ranged from 5.4 to 39.9 gallons per minute.

The steady state flow of the fluid can be followed by the schematic diagram of Figure 4. All piping was of 1-1/2 inch schedule 40 pipe with the exception of the pipe between barrel #1 and barrel #2 which was a 3 inch schedule 40 line. The larger pipe assured adequate delivery rate by gravity from barrel #1 during all runs.

Pressure Sensing Equipment

Two U-tube manometers were used as pressure sensing devices. U-tube manometer #1 was placed across the orifice, and U-tube manometer #2 was placed across the tube bank. Mercury and carbon tetrachloride were used interchangeably as indicating fluids in the tube bank manometer. The other fluid in the manometer was the same as the fluid inside the tube bank. Both manometers were equipped with drain lines.

Orifice Apparatus

The orifice used in this experiment had a diameter of 23/32 of an inch and was 1/8 of an inch thick. The sharp-edged orifice was not built to meet a specific standard.

Fluid Approach Configuration

Two devices were used to break up any jets from the pipe. They were:

1. A 1/8 inch standard mesh screen located at the approach end of the tube bank
2. A long rectangular approach conduit that encases the tube bank, see

Figure 5 on page 16.

Fann V-G Viscometer

The viscometer used in this study was a Fann V-G Model 34 meter. The Fann viscometer is a concentric cylinder apparatus with a stationary inner cylinder. The outer cylinder is rotated at various speeds. Attached to the inner cylinder is a compact torsion spring unit that provides very rapid response and continuous indication of the torque. See Appendix B.

Sodium Carboxymethylcellulose

The power-law non-Newtonian fluid studied was a one per cent solution by weight of high viscosity Driscose (CMC) and water. A one per cent solution of Driscose in water has an apparent viscosity of approximately 2,000 centipoises (7) at low shear rates.

Mixing Apparatus

The primary mixing apparatus was a ASOL Lightning mixer powered by a one-quarter horsepower motor. The Moyno pump was run during the mixing to further assist in mixing.

CHAPTER IV

PROCEDURE

There were two calibration marks inside the bottom barrel. The first mark was 24 inches above the bottom of the bottom barrel and the second mark was 12 inches above the first mark.

The bottom barrel was filled with water to the top mark. Water was then siphoned from the bottom barrel into another vessel until the level of the water reached the bottom mark. The vessel containing the water was then weighed. Later the empty vessel was weighed on the same scales. It was then possible to calculate by difference the weight of the water between the two marks in the barrel.

Calibration of the flow rate versus the angular rotation of the pump rotor was facilitated by the use of a stroboscope. The procedure to calibrate the flow rate was to set the angular velocity (RPM), shut off the valve between the top and bottom barrel and observe the time required for the water level of the bottom barrel to go from the top mark to the bottom mark. The mass flow rate was then calculated by dividing the weight of the water that occupied the space between the two marks by the time required for the water level to go from the top mark to the bottom mark. This procedure was repeated throughout the entire range of angular velocities of the pump rotor. The positive displacement characteristics of the Moyno pump made it possible to use the same flow rate at a corresponding angular velocity of the pump rotor for the CMC

runs as for the water calibration runs, made at the same angular velocities of the pump rotor. Comparison of the CMC and water flow rates on an experimental basis showed that they were equal. Duration of the flow rate calibration runs varied from 31.5 seconds to 233.6 seconds.

The tube bank manometer was filled with carbon tetrachloride under water. The manometer readings were recorded at the angular velocities used for the flow rate calibrations. Prior to each reading the manometer drain lines were opened for approximately 20 seconds to allow air to escape from the manometer lines. There was about a ten to fifteen minute duration between each manometer reading. This period of time was allowed so that the system would come to steady state. During this period random readings were read to substantiate that the system was at steady state. The temperature of the water remained at 25 degrees C throughout all of the series of runs. The flow rate varied from 5.4 gallons per minute to about 39.9 gallons per minute. These runs were made for both the four and eight row tube banks.

The water in the system was drained. Water was added from a smaller container. Each time the water was added, the weight of the water and the container was recorded. When the bottom barrel was full the smaller container was weighed. It was then possible to calculate the weight of the water in the system. Sufficient CMC was weighed out to make the solution in the barrel 1 per cent CMC by weight. The CMC was sprinkled on the surface of the solution while the mixing motor was running and the fluid was circulating through the system.

The orifice manometer was filled with mercury under the CMC solution and the tube bank manometer was filled with carbon tetrachloride. Mercury was used interchangeably with carbon tetrachloride in the tube

bank manometer depending upon the flow rate. The same procedure as for the water runs was used for the CMC runs. The temperature of the CMC solution remained at about 28 degrees C. The difference in temperature from the water runs was due to a change in the season of the year. There were two series of water runs made and six series of CMC runs made.

The specific gravity of the CMC solution was obtained from a Fisher-Davidson Gravitometer. The specific gravity of the CMC solution with respect to water was 1.043. The temperature of the CMC solution at the time of the specific gravity determination was 28 degrees C.

The rheological constants were evaluated by the use of a Fann V-G Model 34 viscometer. CMC solution was taken from the lower barrel of the system to test on the Fann V-G viscometer. The outer spindle of the Fann rotated at 3, 6, 100, 200, 300, and 600 revolutions per minute. Readings that indicated the torque on the inner spindle were recorded at each rotational speed. The temperature of the CMC solution during these readings was 28 degrees C.

CHAPTER V

PRESENTATION AND DISCUSSION OF RESULTS

Friction factors and Reynolds numbers for the water runs were calculated using equations (10) and (4). The calculated f and Re_t values are tabulated in Table I on page 46 for the four row and eight row tube bank arrangements. The raw data for the runs are found in Table VI on page 55.

The Reynolds number-friction factor data for the water runs are compared to the Re_t-f curves for Newtonian fluids as reported by other authors (12, 13, 14) in Figure 6 on page 23. The intention of the comparison of the curves was to insure that conditions and geometries of the tube banks used in this work were consistent with those of previous works. The friction factors in the range of Reynolds numbers do not deviate radically from the friction factors of other investigators in view of the fact that the literature values do not show close agreement. Therefore, it was concluded that the conditions of this work were similar to those of previous work. It is of interest to note that most of the published work in this Reynolds number range is for flow of air across tube banks.

The same equation used to calculate the friction factor for the water runs was used to calculate the friction factor for the CMC solution runs, equation (10). Reynolds numbers were calculated by equation (8), the modified Reynolds number for non-Newtonian flow through a pipe. The

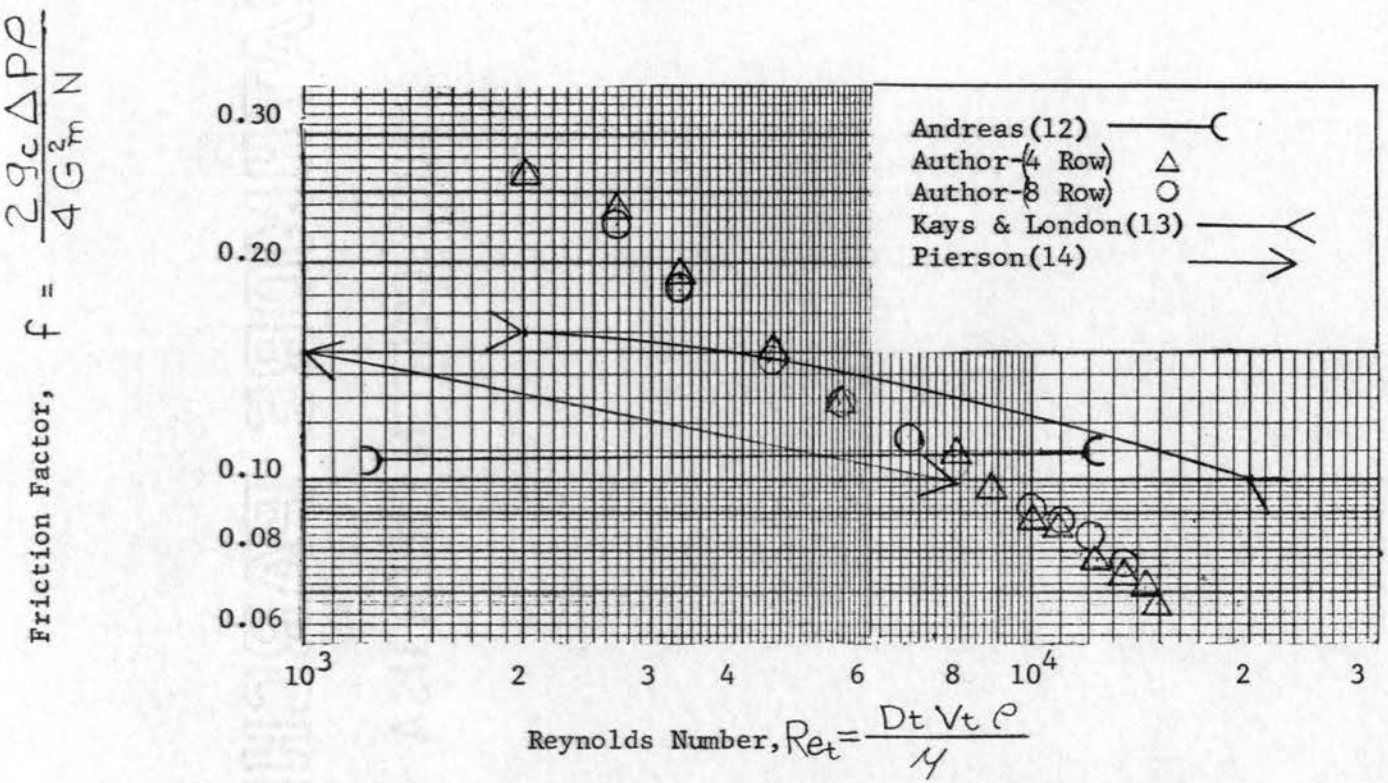

Figure 6. Friction Factor-Reynolds Number Diagram for Flow Across a Staggered Square Tube Bank

numerical values of the friction factors and Reynolds numbers for CMC runs are tabulated in Table II on page 47. The raw data for the CMC runs are found in Table IX on page 60.

Figure 7 on page 25 is a diagram of Re_t versus f comparing the curves of Bergelin et al. (1) and Bell (15) for Newtonian flow across tube banks to the curves for the flow of CMC across tube banks. The Newtonian fluids that Bergelin used in his studies were highly viscous oils. Bergelin studied a staggered square tube bank with a pitch ratio of 1.25. Bell (15) estimated a Reynolds number-friction factor curve for Newtonian fluids flowing across a staggered square tube bank arrangement with a 1.50 pitch ratio. Bell's curve is based on a semi-empirical method suggested by Friedl (16). Bell's curve is within the scatter of the friction factors for the CMC runs at the higher Reynolds numbers investigated. The friction factors of Bell's work were slightly lower than the friction factors of this work at lower Reynolds numbers.

Orifice coefficient-Reynolds number curves for Newtonian fluids and the CMC solution are compared in Figure 8 on page 26. The orifice coefficients for both the Newtonian fluids and the CMC solution were calculated by equation (10). The Newtonian Reynolds numbers were calculated using equation (4). The non-Newtonian Reynolds numbers were calculated using equation (9). The Newtonian Reynolds number-orifice curve can be found in Tuve and Sprenkel (17). The orifice coefficients for the non-Newtonian runs are slightly higher than the Newtonian orifice coefficients.

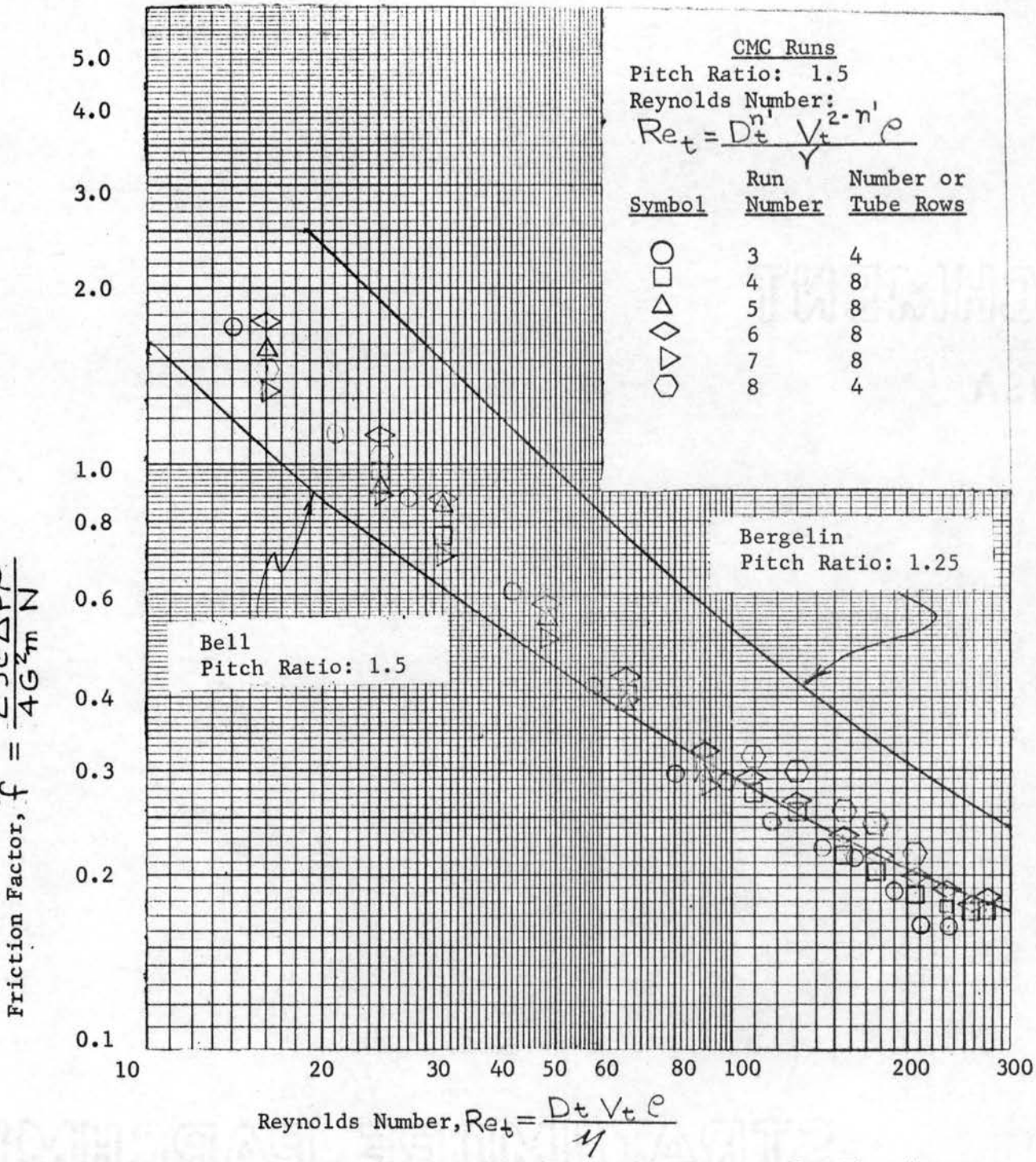

Figure 7. Friction Factor-Reynolds Number Diagram for Flow Across Staggered Square Tube Banks

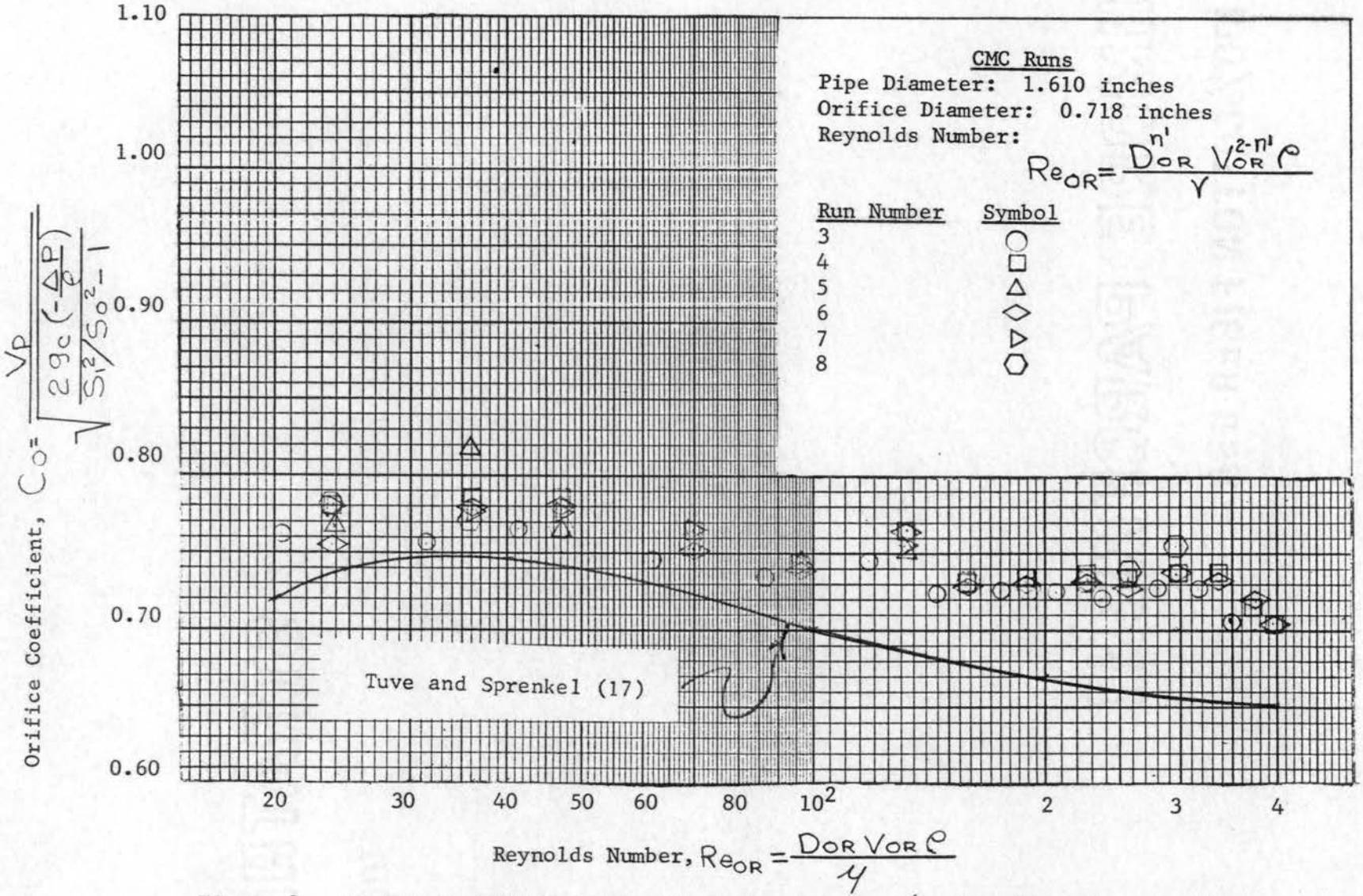

Figure 8. Orifice Coefficient Reynolds Number Diagram for Flow Through an Orifice

CHAPTER VI

EXPERIMENTAL ERRORS

There were six sources of experimental error in this work. The first experimental error involved the flow rate calibration runs. The surface of the water in the bottom barrel did not remain smooth as the water level went from the top mark to the bottom mark. The surface of the water was not smooth because of vibrations of the pump and the motor. The water surface varied by $\pm 1/4$ inches. This error was prevalent at both the top and bottom readings. Other sources of experimental error were the manometer readings, the specific gravity determinations from the Fisher-Davidson gravitometer, the stop watch, geometrical measurements, and the Fann V-G Viscometer readings. The accuracy with which each of these readings can be read are listed below.

Manometer Leg Heights.....$\pm$0.02 Inches

Fisher-Davidson Gravitometer.....$\pm$0.001 Dimensionless

Stop Watch.....$\pm$0.1 Seconds

Fann V-G Viscometer.....$\pm$0.5 Degrees

Tube Diameter.....$\pm$0.002 Inches

Orifice Diameter.....$\pm$0.002 Inches

The experimental errors affected three different quantities: the Reynolds number, the orifice coefficient, and the friction factor. The maximum errors at the highest and lowest flow rates are listed below based on the above tolerances and series number 3 on page 50.

See page 73 for detailed calculations of the maximum errors.

For a given run the maximum error in the calculated value of the Reynolds number is

Test Fluid	Error at Lowest Flow Rate	Error at Highest Flow Rate
Water	±6.3%	±6.1%
1% CMC in Water	±7.7%	±8.0%

The maximum error in the calculated value of the friction factor is

Test Fluid	Error at Lowest Flow Rate	Error at Highest Flow Rate
Water	±10.2%	±11.4%
1% CMC in Water	±10.1%	±10.3%

The maximum error in the calculated value of the orifice coefficient is

Test Fluid	Error at Lowest Flow Rate	Error at Highest Flow Rate
1% CMC in Water	±5.0%	±9.3%

CHAPTER VII

CONCLUSIONS AND RECOMMENDATIONS

Conclusions

The purpose of this study was to determine whether or not a Reynolds number-friction factor diagram for the flow of Newtonian fluids through a tube bank can be applied to pseudoplastic non-Newtonian flow through a similar tube bank. The proposed Reynolds number for non-Newtonian flow through a tube bank was obtained by modifying the Reed and Metzner (8) Reynolds number for non-Newtonian pseudoplastic flow through a pipe. The friction factor-Reynolds number curves for the CMC non-Newtonian runs are in good agreement with the Newtonian friction factor-Reynolds number curve estimated by Bell. It was concluded that for the particular tube bank studied the proposed Reynolds number for non-Newtonian pseuodplastic flow could possibly be valid. It should be pointed out that many similar experiments using different tube bank arrangements should be made before acceptance of the proposed Reynolds number for pseudoplastic non-Newtonian flow through a tube bank can be realized.

A secondary objective was to determine whether or not orifice coefficient-Reynolds number diagrams for Newtonian fluids flowing through an orifice can be applied to non-Newtonian fluids flowing through an orifice. Comparison of the data points of the non-Newtonian flow through the orifice to the curve for Newtonian flow through a similar orifice

indicated that the diagram can be used for approximate design for non-Newtonian flow through the orifice by modifying the Reynolds number. This conclusion is based on the similarity of the two curves taking into consideration that a standardized orifice was not used in these studies.

Recommendations

1. Different tube arrangements should be studied to insure that the modified Reynolds number for non-Newtonian pseudoplastic flow through a tube bank is satisfactory for correlating friction factor data.
2. Make visual study of the flow of CMC through a tube bank so that the phenomenon will be better understood.
3. Make visual study of the flow of CMC through an orifice so that the phenomenon will be better understood.
4. Make more orifice studies to assure that Newtonian Reynolds number-orifice coefficient diagrams can be used for non-Newtonian flow.

BIBLIOGRAPHY

1. Bergelin, O. P., A. P. Colburn, and H. L. Hull, Heat Transfer and Pressure Drop During Viscous Flow Across Unbaffled Tube Banks, University of Delaware Engineering Experiment Station, Bulletin No. 2, (1958).

2. Boucher, D. F. and C. E. Lapple, Chemical Engineering Progress, 44, No. 2, 117 (1948).

3. Ree, F. H., T. H. Ree, and H. Eyring, Ind. Eng. Chem., 50, No. 7, 1036 (1958).

4. Philippoff, W., Kolloid Z., 71, 1-16 (1935).

5. Reiner, M., Deformation and Flow, H. K. Lewis and Company, London, (1949) p. 95-107.

6. Bird, R. B., W. E. Stewart, and E. N. Lightfoot, Transport Phenomena, John Wiley & Sons, Inc., New York, (1960) p. 11.

7. Dr. F. K. Shell, Private Communication, June 8, 1963.

8. Metzner, A. B. and J. C. Reed, A. I. Ch. E. Journal, 1, 434 (1955).

9. Larian, M. G., Fundamentals of Chemical Engineering Operations, Prentice-Hall, Inc., Englewood Cliffs, New Jersey, (1958) p. 47-8.

10. Chilton, T. H. and R. P. Genereaux, Trans. Am. Inst. Chem. Engrs., 29, 161-73 (1933).

11. Gunter, A. Y. and W. Z. Shaw, Trans. Am. Soc. Mech. Engrs., 67, 643-60 (1933).

12. Andreas, J. M., Thesis, Mass. Inst. Tech., (1937).

13. Kays, W. M. and A. L. London, Compact Heat Exchangers, National Press, Palo Alto, California, (1955) p. 91-2.

14. Pierson, O. L., Trans. A. S. M. E., Vol. 59, 573-81 (1937).

15. Dr. K. J. Bell, Private Communication, March 17, 1963.

16. Friedl, P. H., Ph. D. Thesis, Case Institute of Technology, (1960).

17. Tuve, G. L. and R. E. Sprenkel, Instruments, 6, 201 (1933).

18. Bird R. B., W. E. Stewart, and E. N. Lightfoot, Transport Phenomena, John Wiley & Sons, New York, (1960) p. 11.

19. Savins, J. G. and W. R. Roper, API, 7, (1954).

APPENDIX A

DEFINITIONS OF SYMBOLS

APPENDIX A

DEFINITION OF SYMBOLS

B - Integration constant of Eq. (6-B), radians/sec

C_o - Orifice coefficient for incompressible flow, dimensionless

C_1 - Integration constant of Eq. (5-B), $lb_f(sec)^{n-1}$

D_t - Outside tube diameter, ft

D_i - Inside pipe diameter, ft

D_{or} - Orifice diameter, ft

D_1 - Integration constant of Eq. (B-8), $(sec)^{-1}$

f - Friction factor as defined by Chilton and Genereaux, dimensionless, $f = (\Delta P/4N)/(G_m^2/2\rho g_c)$

g_c - Conversion factor 32.17 $lb_m/(lb_f(ft/sec^2))$

G_m - Mass velocity at minimum cross-sectional area to flow, $lb_m/(ft^2 sec)$

K - Constant for non-Newtonian power-law shear stress-shear rate equation, $(lb_f\ sec^{n'})/ft^2$

K' - Fluid consistency index, defined by Eq. (7), $(lb_f\ sec^{n'})/ft^2$

K_i - Fann V-G viscometer constant, cm

L - Length of Fann viscometer bob, cm

M - Angular deflection of Fann V-G viscometer

n' - Flow behavior index defined by Eq. (3), dimensionless

N - Number of major restrictions encountered in flow through the tube bank (one less than the number of rows for a staggered square arrangement), dimensionless

P_d - Diagonal pitch ratio, dimensionless (S_d/D_t)

P_l - Longitudinal pitch ratio, dimensionless (S_l/D_t)

P_t - Transverse pitch ratio, dimensionless (S_t/D_t)

ΔP - Pressure drop across section being considered, lb_f/ft^2

RPM - Angular rotation rate, revolutions per minute

Re_{or} - Reynolds number for flow through an orifice based on the diameter of the orifice, dimensionless

Re_p - Reynolds number for flow through pipe based on the diameter of the pipe, dimensionless

Re_t - Reynolds number for flow through a tube bank based on the outside diameter of a tube, dimensionless

S_d - Diagonal pitch (center-to-center distance from tube in one row to tube in next row), ft

S_l - True longitudinal pitch (distance between centers of successive transverse rows), ft

S_t - Transverse pitch (center-to-center distance between adjacent tubes in a given transverse row), ft

S_{tu} - Minimum cross-sectional area to flow in tube bank, ft^2

S_p - Cross-sectional area inside of pipe, ft^2

S_o - Cross-sectional area of orifice, ft^2

t - Time, sec

V_t - Velocity of fluid in tube bank at minimum cross-sectional area to flow, ft/sec

V_p - Velocity of fluid in pipe, ft/sec

V_l - Velocity of fluid in orifice, ft/sec

V_θ - Velocity in angular direction, ft/sec

V_r - Velocity in radial direction, ft/sec

Z - Vertical height in cylindrical coordinates, ft

Greek Letters

μ - Viscosity, $lb_m/(ft\ sec)$

ρ - Density, lb_m/ft^3

θ - Angle, degrees

γ - Denominator of the generalized Reynolds number defined by Eq. (6), $lb_m/(ft\ sec^{2-n'})$

Ω - Angular rotation, radians per second

$\tau_{r\theta}$ - Flux of θ -momentum through a face perpendicular to the r axis

$\tau_{\theta\theta}$ - Flux of θ -momentum through a face perpendicular to the θ axis

$\tau_{\theta z}$ - Flux of Z-momentum through a face perpendicular to the θ axis

APPENDIX B

EVALUATION OF CONSTANTS FOR NON-NEWTONIAN POWER-LAW SHEAR STRESS-SHEAR RATE EQUATION

APPENDIX B

EVALUATION OF CONSTANTS FOR NON-NEWTONIAN POWER-LAW SHEAR STRESS-SHEAR RATE EQUATION

The System

Consider two vertical concentric circular cylinders. The inner radius of the outer cylinder is designated by r_2. The outer radius of the inner cylinder is r_1. The outer cylinder is rotating at Ω revolutions per minute while the inner cylinder remains stationary. The cylinders are infinitely long, so end effects may be neglected. The fluid between the walls of r_2 and r_1 is a power-law non-Newtonian fluid and is characteristically very viscous (on the order of 2,000 centipoises). A top view of the system is given below.

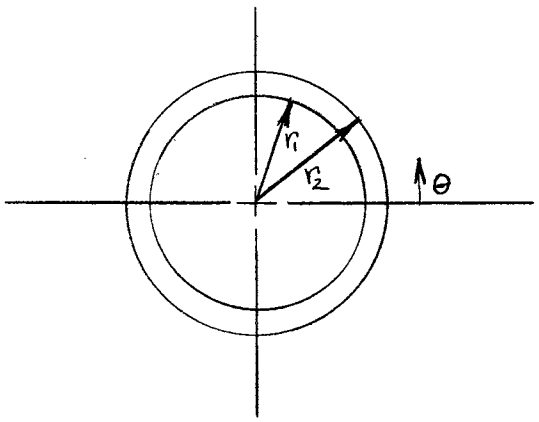

Figure 9. Diagram of Concentric Cylinder Viscometer

Assumptions

1. Incompressible flow
2. No slip at the walls of the cylinders
3. Fluid is in laminar flow (due to high viscosity)
4. No motion in radial direction (r)
5. No motion in vertical direction (Z)
6. Steady state (fully developed flow)
7. No body forces acting on the system in the (θ) direction

Derivation

Motion as described in cylindrical coordinates, in terms of shear stress, is represented by three equations. The first equation describes motion in the radial (r) direction, the second describes motion in the vertical (Z) direction, and the third describes motion in the angular (θ) direction. Since, for this case, there is no motion in the radial (r) direction and in the vertical (Z) directions, the equations describing motion in these directions become trivial.

The equation representing motion in the angular (θ) direction is given by Bird, Stewart, and Lightfoot (18).

$$\rho\left(\frac{\partial V_\theta}{\partial t}+\frac{V_r\,\partial V_\theta}{\partial r}+\frac{V_\theta}{r}\,\frac{\partial V_\theta}{\partial \theta}+\frac{V_r V_\theta}{r}+V_z\,\frac{\partial V_\theta}{\partial z}\right)=$$

$$-\frac{1}{r}\,\frac{\partial P}{\partial \theta}-\left(\frac{1}{r^2}\,\frac{\partial(r^2\tau_{r\theta})}{\partial r}+\frac{1}{r}\,\frac{\partial \tau_{\theta\theta}}{\partial \theta}+\frac{\partial \tau_{\theta z}}{\partial z}\right)+\rho g_\theta \qquad (1\text{-B})$$

Based on the assumptions listed, certain terms of this equation are zero. The steady state assumption requires that any term containing a partial with respect to time be zero. Terms pertaining to motion in

the (r) and (Z) directions must also be zero because of assumptions (4) and (5). There are no ΔP and gravitational effects in the radial direction. The resulting equation is

$$-\frac{1}{r^2}\frac{d(r^2\tau_{r\theta})}{dr}=0 \tag{2-B}$$

For a power-law non-Newtonian fluid the shear stress is related to the shear rate in the following manner.

$$\tau_{r\theta}=-K\left[r\frac{d(V_\theta/r)}{dr}\right]^{n'} \tag{3-B}$$

Substituting $\tau_{r\theta}$ from Eq. (3-B) into Eq. (2-B)

$$-\frac{1}{r^2}\frac{d}{dr}\left[-Kr^2\left[\frac{rd(V_\theta/r)}{dr}\right]^{n'}\right]=0 \tag{4-B}$$

Multiplying both sides of Eq. (4-B) by r^2 and integrating

$$Kr^2\left[r\frac{d(V_\theta/r)}{dr}\right]^{n'}=C_1 \tag{5-B}$$

$$r\frac{d(V_\theta/r)}{dr}=\left(\frac{C_1}{K}\right)^{\frac{1}{n'}}r^{-\frac{2}{n'}} \tag{6-B}$$

Let $B=\left(\frac{C_1}{K}\right)^{\frac{1}{n'}}$

$$r\frac{d(V_\theta/r)}{dr}=Br^{-\frac{2}{n'}} \tag{7-B}$$

Integrating again and rearranging

$$\frac{V_\theta}{r}=-\frac{n'Br^{\frac{-2}{n'}}}{2}+D_1 \tag{8-B}$$

$$V_\theta = -\frac{n' B r^{1-\frac{2}{n'}}}{2} + D_1 r \tag{9-B}$$

The assumption of no slip at the wall postulates that the fluid immediately adjacent to the wall is traveling at the same speed as the wall. Therefore, for the case of a stationary inner cylinder and the outer cylinder rotating at Ω radians per minute, this assumption gives rise to two boundary conditions.

1. At $r = r_1$ $\quad V_\theta = 0$
2. At $r = r_2$ $\quad V_\theta = R_2\Omega$

These boundary conditions are used to evaluate constants resulting from integration B and D_1.

Applying B. C. #1 to Eq. (9-B)

At $r = r_1$ $\quad V_\theta = 0$

$$0 = \frac{-nB r_1^{1-\frac{2}{n'}}}{2} + D_1 r_1$$

$$D_1 = \frac{nB r_1^{-\frac{2}{n'}}}{2} \tag{10-B}$$

Applying B. C. #2 to Eq. (9-B)

At $r = r_2$ $\quad V_\theta = r_2\Omega$

$$r_2\Omega = -\frac{nB r_2^{1-\frac{2}{n'}}}{2} + D_1 r_2 \tag{11-B}$$

Substituting Eq. (10-B) into Eq. (11-B) and solving for constant B,

$$B = \frac{2(r_2 r_1)^{\frac{2}{n'}}\Omega}{n\left[r_2^{\frac{2}{n'}} - r_1^{\frac{2}{n'}}\right]} \tag{12-B}$$

Non-Newtonian shear rate is represented by Eq. (7-B).

Substitution of B from Eq. (12-B) into Eq. (7-B) gives

$$r\frac{d\left(\frac{V_\theta}{r}\right)}{dr} = Br^{-\frac{2}{n'}} \tag{7-B}$$

$$= \frac{2(r_2 r_1)^{\frac{2}{n'}}\Omega r^{-\frac{2}{n'}}}{n'\left(r_2^{\frac{2}{n'}} - r_1^{\frac{2}{n'}}\right)} \tag{13-B}$$

Evaluation of the shear rate where $r = r_1$ gives:

$$r\frac{d\left(\frac{V_\theta}{r}\right)}{dr}\bigg|_{r=r_1} = \frac{2r_2^{\frac{2}{n'}}\Omega}{n'\left(r_2^{\frac{2}{n'}} - r_1^{\frac{2}{n'}}\right)} \tag{14-B}$$

Substitution of Eq. (14-B) into Eq. (3-B)

$$\tau_{r\theta}\Big|_{r=r_1} = -K\left[\frac{2r_2^{\frac{2}{n'}}\Omega}{n'\left(r_2^{\frac{2}{n'}} - r_1^{\frac{2}{n'}}\right)}\right]^{n'} \tag{15-B}$$

Practical Application of Equation (15-B)

The Fann V-G Viscometer is geometrically very similar to the system previously described. The only difference in the two systems is that the cylinders of the Fann are not infinitely long. The end effects are considered to be small and are neglected (19).

The procedure for calculating shear stress on the outer surface of the inner cylinder (r_1) at a specific angular velocity is given by Lapple (2)

$$\tau_{r\theta}\Big|_{r=r_1} = \frac{T}{2\pi r_1^2 L} \tag{16-B}$$

where T is torque and L is the length of the inner cylinder. The torque in Eq. (16-B) is calculated by an equation applicable to the Fann V-G

viscometer.

$$T = K_i M \tag{17-B}$$

T - Torque at the outer surface of the inner cylinder

K_i - Instrument spring constant

M - Angular deflection read directly from Fann V-G Viscometer

Substituting Eq. (17-B) into Eq. (16-B)

$$\tau_{r\theta}\Big|_{r=r_1} = \frac{K_i M}{2\pi r_1^2 L} \tag{18-B}$$

Now substituting Eq. (18-B) into Eq. (15-B)

$$\frac{K_i M}{2\pi r_1^2 L} = -K\left[\frac{2 r_1^{\frac{2}{n'}}\Omega}{n'\left(r_2^{\frac{2}{n'}} - r_1^{\frac{2}{n'}}\right)}\right]^{n'} \tag{19-B}$$

Solving Eq. (19-B) for K

$$K = -\frac{\frac{K_i M}{2\pi r_1^2 L}}{\left[\frac{2 r_1^{\frac{2}{n'}}\Omega}{n'\left(r_2^{\frac{2}{n'}} - r_1^{\frac{2}{n'}}\right)}\right]^{n'}} \tag{20-B}$$

Consider the instance where two torques are found at two corresponding angular velocities for the same fluid. Set K from the first reading equal to K from the second reading:

$$\frac{\frac{-K_i M_1}{2\pi r_1^2 L}}{\left[\frac{2 r_2^{\frac{2}{n'}}\Omega_1}{n'\left(r_2^{\frac{2}{n'}} - r_1^{\frac{2}{n'}}\right)}\right]^{n'}} = \frac{\frac{-K_i M_2}{2\pi r_1^2 L}}{\left[\frac{2 r_2^{\frac{2}{n'}}\Omega_2}{n'\left(r_2^{\frac{2}{n'}} - r_1^{\frac{2}{n'}}\right)}\right]^{n'}} \tag{21-B}$$

which reduces to

$$\frac{M_1}{\Omega_1^{n'}} = \frac{M_2}{\Omega_2^{n'}} \qquad (22\text{-B})$$

Rearranging and taking logarithms

$$n' = \frac{\text{Log}\, M_1 - \text{Log}\, M_2}{\text{Log}\, \Omega_1 - \text{Log}\, \Omega_2} \qquad (23\text{-B})$$

K is then evaluated by substituting the numerical value of n' into Eq. (20-B).

APPENDIX C

EXPERIMENTAL DATA AND CALCULATED RESULTS

TABLE I

CALCULATED FRICTION FACTORS AND REYNOLDS NUMBERS FOR WATER FLOWING THROUGH TUBE BANKS FOUR AND EIGHT ROWS DEEP

Series Number 1 (4 Rows Deep)		Series Number 2 (8 Rows Deep)	
Reynolds Number	Friction Factor	Reynolds Number	Friction Factor
13,300	0.076	14,900	0.069
12,200	0.083	14,300	0.071
11,000	0.088	13,300	0.074
10,000	0.092	12,200	0.077
8,800	0.100	11,000	0.085
7,780	0.106	10,000	0.086
6,770	0.116	8,800	0.096
5,430	0.129	7,780	0.109
4,320	0.149	5,430	0.129
3,260	0.184	4,320	0.150
2,690	0.223	3,260	0.191
2,010	0.262	2,690	0.239
		2,010	0.266

TABLE II

CALCULATED FRICTION FACTORS AND REYNOLDS NUMBERS FOR A ONE PER CENT SOLUTION OF CMC AND WATER FLOWING THROUGH STAGGERED SQUARE TUBE BANKS FOUR AND EIGHT ROWS DEEP

Series Number 3 (4 Rows Deep)		Series Number 4 (8 Rows Deep)	
Reynolds Number	Friction Factor	Reynolds Number	Friction Factor
234	0.162	272	0.175
213	0.172	256	0.173
189	0.189	231	0.178
162	0.211	206	0.187
142	0.222	177	0.202
117	0.248	156	0.216
98	0.288	130	0.258
80	0.292	109	0.276
58	0.417	90	0.308
42	0.601	66	0.403
28	0.867	48	0.547
21	1.122	32	0.756
14	1.709	25	0.980

TABLE II (CONTINUED)

Series Number 5 (8 Rows Deep)

Reynolds Number	Friction Factor
90	0.296
66	0.391
48	0.543
32	0.846
25	0.907
16	1.582

Series Number 6 (4 Rows Deep)

Reynolds Number	Friction Factor
272	0.185
256	0.179
231	0.190
206	0.200
177	0.216
156	0.233
130	0.266
109	0.293
90	0.326
66	0.431
48	0.580
32	0.863
25	1.122
16	1.758

TABLE II (CONTINUED)

Series Number 7 (8 Rows Deep)

Reynolds Number	Friction Factor
90	0.286
66	0.389
48	0.505
32	0.704
25	0.897
16	1.324

Series Number 8 (4 Rows Deep)

Reynolds Number	Friction Factor
206	0.219
177	0.246
156	0.259
130	0.300
109	0.313
90	0.334
66	0.438
48	0.592
32	0.787
25	1.012
16	1.493

TABLE III

CALCULATED ORIFICE COEFFICIENTS AND REYNOLDS NUMBERS FOR

A ONE PER CENT SOLUTION OF CMC IN WATER

Series Number 3		Series Number 4	
Reynolds Number	Orifice Coefficient	Reynolds Number	Orifice Coefficient
3,500	0.705	3,950	0.702
3,150	0.729	3,720	0.716
2,800	0.728	3,350	0.739
2,390	0.720	2,990	0.736
2,090	0.727	2,570	0.735
1,740	0.725	2,260	0.737
1,450	0.721	1,890	0.732
1,190	0.745	1,590	0.731
860	0.735	1,310	0.766
619	0.745	960	0.745
412	0.766	700	0.766
312	0.756	470	0.785
204	0.762	360	0.786
		239	0.780

TABLE III (CONTINUED)

Series Number 5		Series Number 6	
Reynolds Number	Orifice Coefficient	Reynolds Number	Orifice Coefficient
1,307	0.751	3,950	0.705
959	0.744	3,717	0.719
696	0.751	3,354	0.732
470	0.765	2,993	0.736
360	0.819	2,572	0.730
239	0.769	2,263	0.732
		1,887	0.732
		1,588	0.730
		1,307	0.765
		959	0.740
		696	0.756
		470	0.781
		360	0.779
		239	0.754

TABLE III (CONTINUED)

Series Number 7		Series Number 8	
Reynolds Number	Orifice Coefficient	Reynolds Number	Orifice Coefficient
1,307	0.760	2,993	0.755
959	0.746	2,572	0.730
696	0.765	2,263	0.734
470	0.779	1,887	0.730
360	0.776	1,588	0.726
239	0.780	1,307	0.764
		959	0.746
		696	0.755
		470	0.769
		360	0.771
		239	0.781

TABLE IV

WEIGHT OF WATER BETWEEN VERTICAL MARKS IN LOWER BARREL

Date: January 3, 1963
Water Temperature: 24 degrees C

Run Number 1

Weight of vessel and water	188.5 pounds
Weight of dry vessel	14.0 pounds
Weight of water	174.5 pounds

Run Number 2

Weight of vessel and water	189.0 pounds
Weight of dry vessel	14.0 pounds
Weight of water	175.0 pounds

TABLE V

FLOW RATE CALIBRATION

Date: February 3, 1963

Water temperature: 25 Degrees C

Stroboscope Setting	Time required for the water level in the bottom barrel to go from the top mark to the bottom mark		
	Series #1	Series #2	Series #3
RPM	Seconds	Seconds	Seconds
665	31.7	31.9	31.6
650	33.2	32.9	33.0
600	35.4	35.5	35.8
550	38.5	38.9	38.9
500	42.7	43.1	42.9
450	46.9	47.0	47.4
400	53.1	53.5	53.5
350	60.2	60.8	60.5
300	69.4	69.7	69.8
250	86.8	87.2	86.9
200	108.6	108.8	109.1
150	144.3	144.6	144.7
125	174.1	174.1	174.0
Min	233.7	233.9	234.2

TABLE VI

EXPERIMENTAL DATA FOR WATER RUNS

Date:	February 8, 1963
Test fluid:	Water
Orifice manometer fluid:	Mercury
Tube bank manometer fluid:	Carbon tetrachloride
Number of rows of tubes:	8
Series number:	1

Stroboscope	Temperature	Tube Bank Manometer Readings	
		Left	Right
RPM	Degrees C	Inches	Inches
600	25.0	-14.40	14.10
550	25.0	-13.40	13.10
500	25.0	-11.40	11.10
450	25.0	- 9.90	9.65
400	25.0	- 8.35	8.10
350	25.0	- 6.95	6.75
300	25.0	- 5.75	5.60
250	25.0	- 4.10	4.00
200	25.0	- 3.00	2.90
150	25.0	- 2.10	2.05
125	25.0	- 1.75	1.70
Min	25.0	- 1.15	1.10

TABLE VI (CONTINUED)

Date:	February 9, 1963
Test fluid:	Water
Orifice manometer fluid:	Mercury
Tube bank manometer fluid:	Carbon tetrachloride
Number of rows of tubes:	4
Series number:	2

		Tube Bank Manometer Readings	
Stroboscope	Temperature	Left	Right
665	25.0	-7.10	6.85
650	25.0	-6.70	6.50
600	25.0	-6.25	6.20
550	25.0	-6.10	5.80
500	25.0	-5.35	5.15
450	25.0	-4.00	3.90
400	25.0	-3.45	3.35
350	25.0	-3.05	2.95
300	25.0	-2.55	2.40
250	25.0	-1.75	1.70
200	25.0	-1.30	1.25
150	25.0	-0.95	0.90
125	25.0	-0.80	0.78
Min	25.0	-0.50	0.48

TABLE VII

PREPARATION OF A 1% SOLUTION OF CMC AND WATER

Weight of Water in Bottom Barrel

A small container was weighed dry. The container was then filled with water and weighed. The water was then added to the bottom barrel. It was then possible to calculate the weight of the water by the difference in weight. This procedure was repeated until the barrel was full.

Weight of the container: 3 pounds and 0 ounces

Run number	Weight of Container and Water	
	Pounds	
1	44.75	Water Temperature: 25 Degrees C
2	45.75	
3	39.50	
4	47.25	
5	45.25	
6	46.25	
7	43.50	
8	46.50	
9	42.00	
10	44.00	
11	36.00	
Total	480.75	
	-33.00	(Weight of container times the number of runs)
	447.75 Pounds	

TABLE VII (CONTINUED)

Weight of CMC in Bottom Barrel

Weight of container and CMC	2,520 Grams
Weight of empty container	468 Grams
Weigth of CMC in bottom barrel	2,052 Grams

Specific Gravity of the 1% Solution of CMC and Water

The specific gravity of the one per cent solution with reference to water was determined by a Fisher-Davidson Gravitometer. The results are:

Solution temperature: 25 Degrees C

Run number 1	1.045
Run number 2	1.043
Run number 3	1.044

TABLE VIII

EXPERIMENTAL DATA FROM FANN V-G VISCOMETER

Date: June 5, 1963
Temperature: 26 Degrees C

	Deflection of Scale Reading		
	Run #1	Run #2	Run #3
RPM	Degrees	Degrees	Degrees
3	3.1	3.1	3.1
6	5.8	5.8	5.9
100	49.2	48.9	48.7
200	76.5	76.7	76.7
300	97.9	98.0	98.0
600	143.3	143.4	143.7

Fann V-G Constants

Inside diameter of the outer cylinder	1.842 cm
Outside diameter of the inner cylinder	1.725 cm
Length of inner cylinder	3.80 cm
Fann V-G Spring constant	387 Dyne cm/Deg.

TABLE IX

EXPERIMENTAL DATA FOR CMC RUNS

Date:	April 24, 1963
Test fluid:	1% CMC in water
Orifice manometer fluid:	Mercury
Tube bank manometer fluid:	Carbon tetrachloride
Number of rows of tubes:	8
Series number:	3

		Orifice Manometer Reading		Tube Bank Manometer Reading	
Stroboscope	Temperature	Left	Right	Left	Right
RPM	Degrees C	Inches	Inches	Inches	Inches
650	28.0	-11.92	11.69	-15.27	15.90
600	28.0	-10.25	10.13	-14.59	14.02
550	28.0	- 8.61	8.44	-13.61	13.06
500	28.0	- 7.18	7.06	-12.20	11.69
450	28.0	- 5.83	5.74	-10.73	10.22
400	28.0	- 4.61	4.52	- 9.29	8.80
350	28.0	- 3.61	3.52	- 8.43	7.99
300	28.0	- 2.55	2.47	- 6.49	6.10
250	28.0	- 1.71	1.62	- 5.95	5.62
200	28.0	- 1.08	0.99	- 5.46	5.10
150	28.0	- 0.59	0.51	- 4.49	4.16
125	28.0	- 0.42	0.36	- 3.99	3.68
Min	28.0	- 0.26	0.17	- 3.41	3.10

TABLE IX (CONTINUED)

Date: May 29, 1963
Test fluid: 1% CMC in water
Orifice manometer fluid: Mercury
Tube bank manometer fluid: Mercury
Number of rows of tubes: 8
Series number: 4

		Orifice Manometer Reading		Tube Bank Manometer Reading	
Stroboscope	Temperature	Left	Right	Left	Right
RPM	Degrees C	Inches	Inches	Inches	Inches
665	28.0	-13.74	13.73	-1.90	1.88
650	28.0	-11.51	11.47	-1.74	1.69
600	28.0	- 9.98	9.90	-1.55	1.50
550	28.0	- 8.37	8.32	-1.39	1.33
500	28.0	- 6.82	6.81	-1.21	1.15
450	28.0	- 5.60	5.61	-1.07	1.03
400	28.0	- 4.43	4.48	-0.97	0.97
350	28.0	- 3.48	3.52	-0.83	0.79
300	28.0	- 2.38	2.42	-0.70	0.67
250	28.0	- 1.56	1.58	-0.59	0.56
200	28.0	- 0.96	0.99	-0.50	0.49
150	28.0	- 0.52	0.53	-0.40	0.38
125	28.0	- 0.34	0.38	-0.36	0.33
Min	28.0	- 0.20	0.21	-0.30	0.27

TABLE IX (CONTINUED)

Date:	May 29, 1963
Test fluid:	1% CMC in water
Orifice manometer fluid:	Mercury
Tube bank manometer fluid:	Carbon tetrachloride
Number of rows of tubes:	8
Series number:	5

		Orifice Manometer Reading		Tube Bank Manometer Reading	
Stroboscope	Temperature	Left	Right	Left	Right
RPM	Degrees C	Inches	Inches	Inches	Inches
300	28.0	-2.52	2.46	-14.61	15.24
250	28.0	-1.67	1.59	-12.45	12.84
200	28.0	-1.03	1.00	-10.99	11.27
150	28.0	-0.57	0.54	- 9.77	9.99
125	28.0	-0.36	0.30	- 7.00	7.46
Min	28.0	-0.26	0.16	- 6.92	7.14

TABLE IX (CONTINUED)

Date: June 4, 1963
Test fluid: 1% CMC in water
Orifice manometer fluid: Mercury
Tube bank manometer fluid: Mercury
Number of rows of tubes: 8
Series number: 6

		Orifice Manometer Reading		Tube Bank Manometer Reading	
Stroboscope RPM	Temperature Degrees C	Left Inches	Right Inches	Left Inches	Right Inches
665	28.0	-13.70	13.54	-2.01	1.99
650	28.0	-11.52	11.41	-1.80	1.74
600	28.0	- 9.96	9.85	-1.64	1.60
550	28.0	- 8.34	8.29	-1.49	1.42
500	28.0	- 6.93	6.89	-1.28	1.25
450	28.0	- 5.68	5.67	-1.16	1.11
400	28.0	- 4.50	4.49	-1.01	0.99
350	28.0	- 3.50	3.49	-0.88	0.84
300	28.0	- 2.43	2.40	-0.74	0.71
250	28.0	- 1.65	1.62	-0.63	0.60
200	28.0	- 1.00	1.00	-0.54	0.51
150	28.0	- 0.51	0.55	-0.46	0.43
125	28.0	- 0.36	0.38	-0.41	0.38
Min	28.0	- 0.21	0.23	-0.37	0.32

TABLE IX (CONTINUED)

Date:	June 6, 1963
Test fluid:	1% CMC in water
Orifice manometer fluid:	Mercury
Tube bank manometer fluid:	Carbon tetrachloride
Number of rows of tubes:	8
Series number:	7

		Orifice Manometer Reading		Tube Bank Manometer Reading	
Stroboscope	Temperature	Left	Right	Left	Right
RPM	Degrees C	Inches	Inches	Inches	Inches
300	28.0	-2.41	2.48	-14.40	14.49
250	28.0	-1.60	1.63	-12.65	12.49
200	28.0	-0.96	1.00	-10.49	10.21
150	28.0	-0.51	0.55	- 8.40	8.04
125	28.0	-0.36	0.38	- 7.37	6.93
Min	28.0	-0.20	0.21	- 6.08	5.69

TABLE IX (CONTINUED)

Date: June 8, 1963
Test fluid: 1% CMC in water
Orifice manometer fluid: Mercury
Tube bank manometer fluid: Carbon tetrachloride
Number of rows of tubes: 4
Series number: 8

		Orifice Manometer Reading		Tube Bank Manometer Reading	
Stroboscope	Temperature	Left	Right	Left	Right
RPM	Degrees C	Inches	Inches	Inches	Inches
550	28.0	-7.96	7.93	-15.30	15.63
500	28.0	-6.92	6.89	-13.89	14.00
450	28.0	-5.67	5.66	-12.25	12.25
400	28.0	-4.52	4.49	-10.97	10.92
350	28.0	-3.52	3.51	- 8.94	8.92
300	28.0	-2.43	2.41	- 7.23	7.21
250	28.0	-1.62	1.60	- 6.05	6.09
200	28.0	-1.01	1.00	- 5.19	5.20
150	28.0	-0.54	0.56	- 3.90	3.98
125	28.0	-0.37	0.38	- 3.42	3.50
Min	28.0	-0.21	0.20	- 2.80	2.89

APPENDIX D

SAMPLE CALCULATIONS

APPENDIX D

SAMPLE CALCULATIONS

The following information must be known about the Fann V-G Model 34 Viscometer to evaluate the constants of the power-law equation:

r_1 1.725 cm

r_2 1.842 cm

L 3.80 cm

K_i 387 Dyne-cm/deg.

Evaluation of the Constants for Non-Newtonian Power-Law Shear Stress-Shear Rate Equation

The following sample calculation will be based on series number 6 with a setting of 665 RPM. The time for the water in the bottom barrel to go from the top mark to the bottom mark was 31.5 seconds for this setting, Table V page 54. There were 8 rows of tubes in the tube bank, each tube being 1/4 of an inch in diameter. The orifice manometer readings were -13.70 and 13.54 inches of mercury. The tube bank manometer readings were -2.01 and 1.99 inches of mercury. The manometer readings are found in Table IX on page 60. The Fann viscometer readings were

RPM	3	6	100	200	300	600
Deflection (Degrees)	3.1	5.8	48.9	76.7	98.0	143.4

The exponent to the power law shear stress equation is evaluated by

Eq. (23-B).

$$n' = \frac{\text{Log } M_{600} - \text{Log } M_{100}}{\text{Log } \Omega_{600} - \text{Log } \Omega_{100}}$$

$$= \frac{\text{Log } 143.4 - \text{Log } 48.9}{\text{Log } 600 - \text{Log } 100} \qquad (23\text{-B})$$

$$= 0.6003$$

The numerical value of n' with the numerical value of M_{600} are substituted into Eq. (20-B) to evaluate K.

$$K = \frac{\frac{Ki\,M}{2\pi r_2^{\frac{2}{n'}} L}}{\left[\frac{2 r_2^{\frac{2}{n'}} \Omega}{n'\left(r_2^{\frac{2}{n'}} - r_1^{\frac{2}{n'}}\right)}\right]^{n'}} \qquad (20\text{-B})$$

$$= 0.3819 \text{ lbf/ft}^2$$

Evaluation of the Reynolds Numbers for Non-Newtonian Flow Through a Tube Bank and for Flow Through an Orifice

K' is evaluated by substituting numerical values of the constants of the shear stress-shear rate power-law equation into Eq. (7).

$$K' = K\left(\frac{3n'+1}{4n'}\right)^{n'}$$

$$= 0.3819\left(\frac{3 \times 0.6003 + 1}{4 \times 0.6003}\right)^{0.6003} \qquad (7)$$

$$= 0.0286$$

Gamma (Υ) is then evaluated by substituting the values of K' and n into Eq. (6).

$$\Upsilon = K' g_c 8^{n'-1}$$

$$= 32.2\left(\frac{\text{lbm ft}}{\text{lbf sec}^2}\right) 0.0286 \left(\frac{\text{lbf sec}^{n'}}{\text{ft}^2}\right) 8^{0.6003-1} \qquad (6)$$

$$= 0.401 \text{ lbm/ft sec}^{2-n'}$$

The numerical values of n' and gamma (γ) are common to both the Reynolds numbers for flow through a tube bank and the Reynolds number for flow through an orifice for the same non-Newtonian solution (CMC). Eq. (8) is the Reynolds number equation for non-Newtonian flow through a tube bank.

$$Re_t = \frac{D_t^{n'} V_t^{2-n'} \rho}{\gamma} \tag{8}$$

The V_t term is the velocity of the non-Newtonian fluid at the point of minimum cross-sectional area to flow. The minimum cross-sectional area to flow for a staggered square tube bank arrangement occurs along the diagonals as shown in Figure 10.

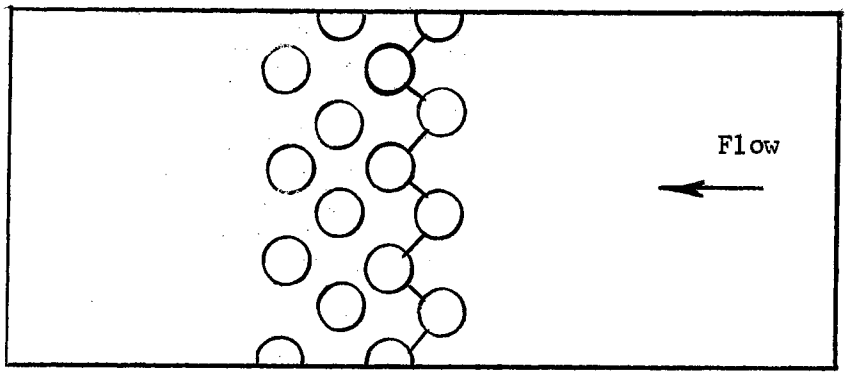

Figure 10. Diagram of the Minimum Cross-Sectional Area to Flow for a Staggered Square Tube Bank

The minimum cross-sectional area to flow is calculated below.

$$StU = \frac{2\,in(0.375\,in - 0.25\,in) \times 7\,Openings}{Opening}\left(\frac{ft^2}{144\,in^2}\right)$$

$$= 0.0121\,ft^2$$

The velocity of the CMC solution flowing through the minimum cross-sectional area to flow is the

$$V_t = \left(\frac{175\,lbm}{35\,Sec}\right)\left(\frac{ft^3}{62.4 \times 1.043\,lbm}\right)\left(\frac{1}{0.0121\,ft^2}\right)$$

$$= 7.36\,ft/sec$$

Eq. (8) with numerical substitution

$$Re_t = \frac{\left(\frac{1/4\,in}{12\,in/ft}\right)^{0.6003}\left(\frac{7.36\,ft}{Sec}\right)^{2-0.6003}\left(\frac{62.4 \times 1.043\,lbm}{ft^3}\right)}{0.401\,lbm/ft\,sec^{2-0.6003}}$$

$$= 272$$

The velocity of CMC flowing through the 23/32 of an inch diameter orifice is

$$V_{OR} = \left(\frac{175\,lbm}{31.5\,Sec}\right)\left(\frac{ft^3}{62.4 \times 1.043\,lbm}\right)\left(\frac{4}{\pi(23/32\,in)^2}\right)\left(\frac{144\,in^2}{ft^2}\right)$$

$$= 31.6\,ft/sec$$

The Reynolds number for flow of CMC through the orifice is

$$Re_{OR} = \frac{\left(\frac{23/32\,in}{12\,in/ft}\right)^{0.6003}\left(\frac{31.6\,ft}{Sec}\right)^{2-0.6003}\left(\frac{62.4 \times 1.043\,lbm}{ft^3}\right)}{0.401\,lbm/ft\,sec^{2-0.6003}}$$

$$= 3,950$$

Evaluation of the Friction Factor for Flow of CMC

Across the Tube Bank

The pressure difference equation for a fluid manometer is written below

$$\Delta P = (\rho_{\text{Mano. Fluid}} - \rho_{\text{Test Fluid}})(Z_2 - Z_1)$$

$$= \frac{(13.546 - 1.043) \times 62.4 \text{ lbm/ft}^3 (1.99 \text{ in} + 2.01 \text{ in})}{12 \text{ in/ft}}$$

$$= 260 \text{ lb/ft}^2$$

The mass velocity through the tube bank is

$$G_M = \frac{W}{t S_{tu}}$$

$$= \frac{175 \text{ lbm}}{31.5 \text{ sec } 0.0121 \text{ ft}^2}$$

$$= 460.4 \text{ lbm/ft}^2 \text{ sec}$$

The numerical values calculated above are then substituted into Eq. (9)

$$f = \frac{2 g_c \Delta P \rho}{4 G_M^2 N} \tag{9}$$

where N is 1 less than the number of tube rows.

$$f = \frac{2 \left(\frac{32.2 \text{ lbm ft}}{\text{lbf sec}^2}\right)\left(\frac{260 \text{ lbf}}{\text{ft}^2}\right)\left(\frac{62.4 \times 1.043 \text{ lbm}}{\text{ft}^3}\right)}{4 (460.4 \text{ lbm/ft}^2 \text{ sec})^2 7}$$

$$= 0.185$$

Evaluation of the Orifice Coefficient

The pressure drop across the orifice is

$$\Delta P = (\rho_{\text{Mano. Fluid}} - \rho_{\text{Test Fluid}})(Z_2 - Z_1)$$

$$\Delta P = \frac{(13546 - 1.043) \times 62.4\ \text{lbm/ft}^3 (13.54\ \text{in} + 13.70\ \text{in})}{12\ \text{in/ft}}$$

$$= 1{,}771.0\ \text{lbf/ft}^2$$

The velocity of the CMC solution flowing through the 1-1/2 inch schedule 40 pipe is

$$V_P = \frac{175\ \text{lbm}}{31.5\ \text{Sec}(62.4 \times 1.043\ \text{lbm/ft}^3)\, 0.01414\ \text{ft}^2}$$

$$= 6.03\ \text{ft/sec}$$

The information above is then substituted into Eq. (10).

$$C_o = \frac{V_P}{\sqrt{\dfrac{2 g_c \left(\dfrac{-\Delta P}{\rho}\right)}{\dfrac{S_1^2}{S_o^2} - 1}}} \qquad (10)$$

$$= \frac{6.03\ \text{ft/sec}}{\sqrt{\dfrac{2\left(\dfrac{32.2\ \text{lbm ft}}{\text{lbf Sec}^2}\right)\left(\dfrac{-1{,}771.0\ \text{lbf/ft}^2}{62.4 \times 1.043\ \text{lbm/ft}^3}\right)}{\dfrac{(1.610)^4}{(23/32)^4} - 1}}}$$

$$= 0.705$$

Evaluation of the Maximum Experimental Error at the Lowest Flow Rate

The calculations below are based on Series number 3 at minimum RPM and the tolerances listed on page 27 for CMC.

Maximum Experimental Error for n' and γ

From page 59 $M_{100} = 48.9 \pm 0.5$ degrees

$$\% \text{ Error} = \frac{\log 49.4 \text{ degrees} - \log 48.9 \text{ degrees}}{\log 48.9 \text{ degrees}}$$

$$= \pm 0.65$$

Maximum Experimental Error in Reading Liquid Level in Barrel

$$\% \text{ Error} = \frac{2 \pi r^2 \Delta L \ 100}{\pi r^2 L}$$

$$= \frac{2(\pm 0.25 \text{ inches}) \ 100}{12 \text{ inches}}$$

$$= \pm 4.16$$

Maximum Experimental Error in Measuring Diameter of Tubes

$$D_t = 0.25 \pm 0.001 \text{ inches}$$

$$\% \text{ Error} = \frac{\pm 0.001 \text{ inches } 100}{0.25 \text{ inches}}$$

$$= \pm 0.40$$

Maximum Experimental Error in Measuring Diameter of Orifice

$$D_{or} = 23/32 \pm 0.001 \text{ inches}$$

$$\% \text{ Error} = \frac{\pm 0.001 \text{ inches } 100}{23/32 \text{ inches}}$$

$$= \pm 0.09$$

Maximum Experimental Error in Measuring Specific Gravity

$$\text{Sp. Gr.} = 1.043 \pm 0.001$$

$$\% \text{ Error} = \frac{\pm 0.001 \ (100)}{1.043}$$

$$= \pm 0.09$$

Maximum Experimental Error in Reading the Stop Watch

$$t = 233.6 \pm 0.1 \text{ seconds}$$

$$\% \text{ Error} = \frac{\pm 0.1 \text{ seconds } 100}{233.6 \text{ seconds}}$$

$$= \pm 0.05$$

Maximum Experimental Error in Reading Orifice Manometer

$$(Z_1 + Z_2) = 0.43 \pm 0.02 \text{ inches}$$

$$\% \text{ Error} = \frac{\pm 0.02 \text{ inches/leg (2 legs) } 100}{0.43 \text{ inches}}$$

$$= \pm 9.32$$

Maximum Experimental Error in Reading Tube Bank Manometer

$$(Z_1 + Z_2) = 6.51 \pm 0.02 \text{ inches}$$

$$\% \text{ Error} = \frac{\pm 0.02 \text{ inches/leg (2 legs) } 100}{6.51 \text{ inches}}$$

$$= \pm 0.61$$

The above experimental errors for the lowest flow rate affected three quantities: the Reynolds number, the orifice coefficient, and the friction factor. The maximum errors contained by these quantities will be presented.

Maximum Error in the Reynolds Number at the Lowest Flow Rate for CMC

$$Re_t = \frac{D_t^{n'} V_t^{2-n'} \rho}{\gamma}$$

Term	Method	Numerical	Error
$D_t^{n'}$	n'(% Error D_t)	0.6003($\pm$0.40%)	$\pm$0.24%
$V_t^{2-n'}$	(2-n')(% Error D_t)	(2-0.6003)($\pm$0.40%)	$\pm$0.56%
	(2-n')(% Error Level in Barrel)	(2-0.6003)($\pm$4.16%)	$\pm$5.82%
	(2-n')(% Error t)	(2-0.6003)($\pm$0.05%)	$\pm$0.07%

ρ	% Error Sp. Gr.	±0.40%	±0.40%
γ	% Error γ	±0.65%	±0.65%
			±7.7%

Maximum Error in the Friction Factor at the Lowest Flow Rate

$$f = \frac{2\Delta P g_c \rho}{4 G_m^2 N}$$

Term	Method	Numerical	Error
ΔP	% Error ΔP		±0.61%
ρ	% Error Sp. Gr.		±0.09%
G_m	2(% Error D_t)	2(±0.40)	±0.80%
	2(% Error t)	2(±0.05%)	±0.10%
	2(% Error Level in Barrel)	2(±4.16%)	±8.32%
	2(% Error Sp. Gr.)	2(±0.09%)	±0.18%
			±10.1%

Maximum Error in the Orifice Coefficient at the Lowest Flow Rate

$$C_o = \frac{V_p}{\sqrt{\frac{2 g_c \left(\frac{-\Delta P}{\rho}\right)}{S_i^2/S_o^2 - 1}}}$$

Term	Method	Numerical	Error
V_p	% Error D_{or}	±0.14%	±0.14%
	% Error t	±0.05%	±0.05%
	% Error Level in Barrel)	±4.16%	±4.16%
ΔP	1/2(% Error $(Z_1 + Z_2)$)	1/2(±9.32%)	±4.66%
S_o	2(% Error D_{or})	2(±0.14%)	±0.28%
ρ	1/2(% Error Sp. Gr.)	±0.09%	±0.09%
			±9.4%

VITA

Carlyn Grant Cruzan

Candidate for the Degree of

Master of Science

Thesis: NON-NEWTONIAN FLUID FLOW THROUGH A STAGGERED SQUARE TUBE BANK

Major Field: Chemical Engineering

Biographical:

Personal Data: Born in Stillwater, Oklahoma May 10, 1938, the son of Charles Grant and Leonore Scott Cruzan.

Education: Attended grade school at Bartlesville, Oklahoma; graduated from College High School of Bartlesville, Oklahoma June, 1956; graduated from the University of Oklahoma; received the degree of Bachelor of Science in Chemical Engineering June, 1961; graduate study has been at Oklahoma State University since 1961; completed the requirements for the Master of Science degree in August, 1964.

Professional Experience: Employed as a process engineer with Phillips Petroleum Company during the summer of 1960; employed Cities Service Petroleum Company as a Junior Engineer during the month of August, 1961; employed as teaching assistant, School of Chemical Engineering, Oklahoma State University during the school year 1961-1962; employed as materials engineer with Ling-Temco-Vought, 1964.